

MgB₂ superconducting thin films grown by magnetron sputtering

S. ULUCAN, L. OZYUZER*, S. OKUR

Department of Physics, Izmir Institute of Technology, Urla, 35430, Izmir, Turkey

In this study, we report the growth and properties of MgB₂ thin films on polycrystalline Al₂O₃ substrates. A composite MgB₂ target was produced by MgB₂ and Mg powder mixing, using a hot pressing technique. MgB₂ thin films were grown on Al₂O₃ substrates by d.c. magnetron sputtering, without heating the substrate. To enhance the superconducting properties of the as-grown films and to increase the crystal quality, an *ex-situ* anneal process was applied. The crystal structure of the thin films was determined by X-ray diffraction. The resistivity versus temperature of the deposited MgB₂ thin films was studied to examine the transition temperatures of the films under various magnetic fields. The effects of the annealing temperature and annealing time on the electrical properties of MgB₂ thin films are revealed.

(Received November 1, 2006; accepted December 21, 2006)

Keywords: MgB₂, Superconductivity, Thin films, Magnetron sputtering

1. Introduction

The discovery of superconductivity in the intermetallic compound MgB₂ (39 K) in 2001 [1] raised great interest in it for electronic applications. It has the highest transition temperature, T_c , among the intermetallic compounds, and obeys the *BCS* predictions of superconductivity as a phonon-mediated superconductor material [2, 3]. MgB₂ is a potential candidate for superconducting electronics applications because of its high T_c , as well as its large coherence length (ξ_0), high critical current density (J_c) and high upper critical magnetic field (H_{c2}) values, as summarized by Bueza and Yamashita [4]. Electronic device fabrication requires high quality thin film growth of MgB₂. Growth of MgB₂ thin films has some obstacles such as the high volatility of Mg and its high oxidation sensitivity. Therefore, knowing the phase diagram of Mg-B system is very important for good quality thin film growth [5]. In order to deposit high quality MgB₂ superconducting thin films, the commonly used techniques are pulsed laser deposition (PLD) [6], molecular beam epitaxy (MBE) [7], evaporation techniques [8] and hybrid physical-chemical vapor deposition [9]. Since the electronics industry requires low operation costs, magnetron sputtering is also a widely studied method for the deposition of MgB₂ thin films. This method includes DC magnetron sputtering [10], RF magnetron sputtering with a single MgB₂ source [11] and co-sputtering with two sources (Mg and B targets) [12]. To enhance the structural and superconducting properties of deposited MgB₂ thin films by magnetron sputtering, several annealing processes have been developed [13].

In addition to these, the lattice parameter of the substrate is another main parameter for sputtering high quality MgB₂ superconducting thin films. Generally, Al₂O₃, MgO, SiC, LaAlO₃ and SrTiO₃ substrates have been used. The main properties of these substrates [14] and the common substrate interaction with MgB₂ are reported elsewhere [15].

In this study, the fabrication of a MgB₂/Mg sputtering target and MgB₂ superconducting thin films prepared by a two step growth technique (deposition by high vacuum magnetron sputtering system and an *ex-situ* anneal process) has been accomplished. The highest T_c onset values are obtained for MgB₂ thin films prepared by a magnetron sputtering system, as an outcome of the present study.

2. Experimental

We used three main steps for the growth of superconducting MgB₂ thin films. These were the production of a single MgB₂ sputtering target, growth of thin films by high vacuum magnetron sputtering system and an *ex-situ* annealing process. Firstly, 15 MgB₂/Mg (0.3 cm height and 1.5 cm radius) composite pellets were fabricated under 0.5 GPa pressure in a metallic dye at 500 °C for 1 hour, in air [16]. Commercially available MgB₂ (Alfa Aesar) and Mg powders (-325 mesh) (99.99% purity) were used to prepare composite pellets. The weight ratio of the homogeneously mixed powders was 80% MgB₂ and 20% Mg. In order to adjust the dimensions of the sputtering target for the system, they were located on a Mg disc (3 mm height and 50 mm radius). Fig. 1 shows a schematic diagram of the fabrication MgB₂/Mg composite target.

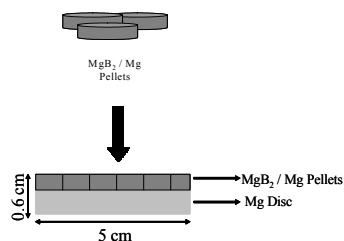


Fig. 1. Fabrication schematic of the MgB_2/Mg composite target.

A schematic diagram of the high vacuum magnetron sputtering system is shown in Fig. 2. The base pressure of the system was kept below 2.0×10^{-6} Torr, using a turbo molecular pump. To create the plasma, Ar gas was used (99.99%). The deposition pressure was 2.5 mTorr and the Ar gas flow was 20 sccm as controlled by a MKS gas flow controller and baratron. Depositions were performed in two steps on polycrystalline Al_2O_3 substrates. The first was the pre-sputtering step, to remove contamination of the target surface over a 30 minute period. The second was the thin film 3 hour deposition step. In the pre-sputtering process, 30 W dc power and 72 mA current were applied. Then the shutter was opened, the dc power and applied current were raised to 50 W and 120 mA. All films had same thickness of $\sim 2 \mu\text{m}$.

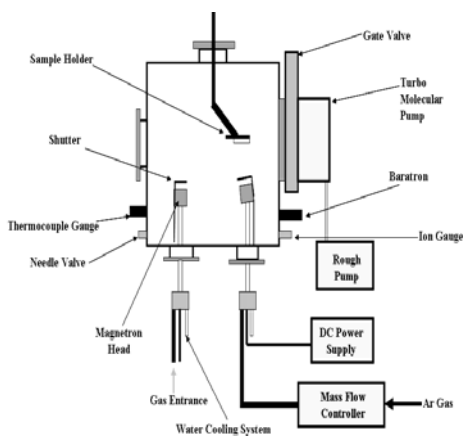


Fig. 2. The schematic of the high vacuum magnetron sputtering system.

The last step for the fabrication of MgB_2 thin films was *ex-situ* annealing. All samples were annealed for various temperatures (625 and 650 °C) and durations (20 and 30 minutes). To perform the annealing process, a high temperature (1200 °C) tube furnace was used. As-grown films were annealed in quartz tubes under an Ar gas (%99.99 purity) flow. The tube furnace reached the annealing temperature at a rate of 20 °C/min. We waited until the system reached room temperature under an Ar gas flow before removing the annealed samples.

In order to obtain the crystal structure of the prepared films, X-ray diffraction was used. For this purpose, Philips™ XRD equipment was operated using $\text{Cu K}\alpha$ radiation. The temperature dependence of the resistance of the deposited MgB_2 thin films, from 300 to 10 K, was studied to obtain the transition temperatures of the films under various magnetic fields (0, 3 and 6 T). This low temperature characterization was performed in a cryogenic free magnet system.

3. Results and discussion

Fig. 3 shows XRD patterns of annealed samples at temperatures of 625 and 650 °C, and for different annealing durations of 20 and 30 minutes. The intensity of each pattern was normalized with respect to their maximum. In the same graph, the pattern of commercial MgB_2 powder (Alfa-Aesar, 98.5%) is presented for comparison. To better understand the XRD results, the XRD pattern of the Al_2O_3 substrate was subtracted from the data. As-grown films have an amorphous structure, so that no crystal peak was detected in XRD. After an *ex-situ* annealing process, all films showed crystallinity in their XRD patterns. The main phase of all samples is MgB_2 which is detected at a $2\theta=42.5^\circ$ position with (101) orientation. Increasing annealing temperature and duration made this peak more detectable. MgB_2 (102) and MgO (220) peaks were detected for all samples around $2\theta=63^\circ$. These peaks are located very close to each other, so it is difficult to distinguish between them. The main MgO (200) peak occurred at $2\theta=43^\circ$, after increasing the annealing time. This peak is more observable for the 30 minutes annealed sample than for the 20 minutes ones. The main reasons for the presence of MgO in our films are the high oxidation sensitivity of Mg even at low temperature, and impurities in the Ar gas (99.99% purity) which was used during the annealing process. The XRD results showed that the *ex-situ* annealing process developed the crystal structure of the MgB_2 thin films.

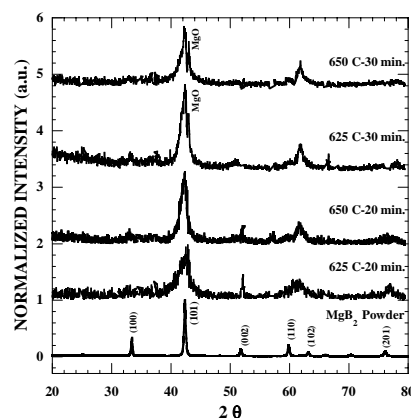


Fig. 3. XRD results for annealed films and MgB_2 powder.

In order to measure the superconducting properties of the samples, four point measurements were done from

room temperature to low temperatures. The room temperature resistivities of all samples were found to be in the mΩ range. Fig. 4 shows the temperature dependence of the normalized resistivity of the films, because the normalization provides a better comparison of the superconducting transition. As-grown films did not show a superconducting transition at low temperatures, because of the amorphous structure. After the annealing process, all samples showed superconducting behavior. The T_c^{Onset} values of all samples were found to be close to each other. The best transition temperature was observed for a sample annealed at 625 °C for 20 min. at $T_c^{\text{Onset}} = 30.5$ K. The other T_c^{Onset} values of the annealed samples were between 27 and 30 K. It was observed that increasing the annealing duration from 20 to 30 minutes reduced the T_c^{Onset} values of the samples, due to oxidation of the Mg even under an Ar gas flow. In addition, the best superconducting transition width (ΔT values, temperature change for a 10%–90% resistivity drop) was observed for the 625°C-20 min. sample, which exhibited $\Delta T = 3.8$ K. In the 20 minute annealed sample, this value increased from 3.8 K to 7.7 K, due to the increased annealing to 7.7 K, due to the increased annealing temperature.

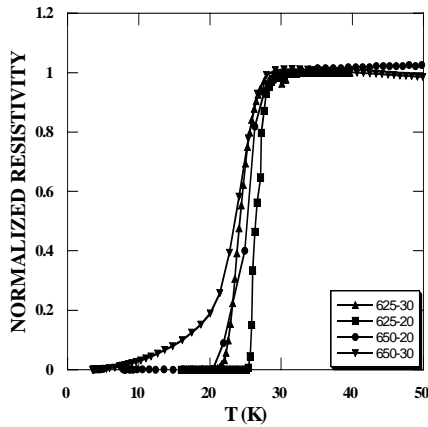


Fig. 4. R-T results for annealed films.

Similarly, ΔT increased from 5.5 K to 13.5 K in the 30 minute annealed samples, with increasing temperature. For the 650 °C-30 min. sample, a tail was observed after the commencement of the superconducting transition. This showed very large superconducting transition width. Considering the XRD results for the 650 °C-30 min. sample, the MgO phase can be responsible for this large transition width. Generally, all samples showed a superconducting transition at various T_c below the bulk value of MgB₂ (39 K). The main reasons of this behavior can be explained as the decomposition of MgB₂ during the deposition process, poor crystallinity even after *ex-situ* annealing and the nonhomogenous superconducting volume of the films.

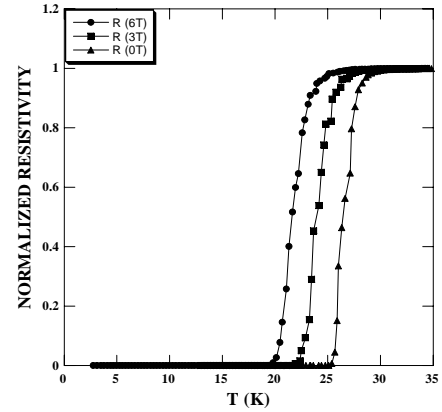


Fig. 5. R-T results for 625 °C-20 min annealed films under various magnetic fields.

The temperature dependence of the resistivity was measured under various magnetic fields (0, 3 and 6 T), in order to obtain the upper critical magnetic field of the films. Fig. 5 shows the normalized resistivity versus temperature for a 625 °C-20 min. sample, under various magnetic fields. Since MgB₂ obeys the BCS prediction [2, 3], we determined the upper critical magnetic field, B_{c2} , for the prepared MgB₂ thin films. The upper critical field at T is given by,

$$B_{c2}(T) = B_{c2}(0) [1 - (T/T_c)^2] \quad (1)$$

Since we can only apply fields up to 6 Tesla, we predicted the upper critical magnetic field of the superconducting MgB₂ films using extrapolation. Fig. 6 shows the T_c values of the films, and fits that were founded on equation 1. As seen, the upper critical magnetic field for the 20 minute annealed sample is 17 T and 19 T for the 30 minute annealed sample. These predictions for the calculated upper critical magnetic field for our MgB₂ thin films are in good agreement with the work of Bueza et al. [4].

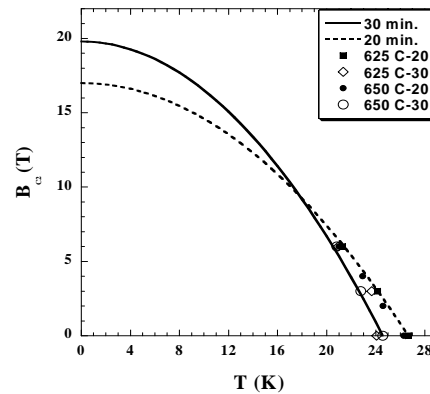


Fig. 6. Upper critical magnetic field versus temperature.

4. Conclusion

A composite, MgB₂/Mg sputtering target for a magnetron sputtering system was successfully produced by MgB₂ and Mg powder mixing with a hot pressing process. MgB₂ thin films were grown by magnetron sputtering without substrate heating. It was found that the as-grown films were not superconductors, and *ex-situ* annealing was necessary to enhance the crystal structure and superconducting properties. However, *ex-situ* annealing also created insulator phases such as MgO. The results indicate that MgB₂ decomposes during the sputtering, and in-situ heating of the substrate can provide better superconducting characteristics, such as a higher T_c and upper critical field for the as-grown films.

Acknowledgments

This research is supported by TUBITAK (Scientific and Technical Research Council of Turkey) project number TBAG-2031. L.O. acknowledges support from Turkish Academy of Sciences, in the framework of the Young Scientist Award Program (LO/TUBA-GEBIP/2002-1-17).

References

- [1] J. Nagamatsu, N. Nakagawa, T. Muranaka, Y. Zenitani, J. Akimitsu, *Nature* **410**, 63 (2001).
- [2] D. G. Hinks, H. Claus, J. D. Jorgenson, *Nature* **411**, 457 (2001).
- [3] T. Yildirim, O. Gulseren, J. W. Lynn, C. M. Brown, T. J. Oldovic, Q. Huang, N. Rogado, K. A. Regan, M. A. Hayward, J. S. Slusky, T. He, M. K. Haas, P. Khalifah, K. Inumaru, R. J. Cava, *Phys. Rev. Lett.* **87**, 3 (2001).
- [4] C. Bueza, T. Yamashita, *Supercond. Sci. Technol.* **14**, R 115 (2001).
- [5] Z. K. Lui, D. G. Scholm, Q. Li, X. X. Xi, *Appl. Phys. Lett.* **78**, 23 (2001).
- [6] A. Brikman, D. Veldhuis, D. Mijatovic, G. Rjinders, D. H. A. Blank, H. Hilgenkamp, H. Rogalla, *Appl. Phys. Lett.* **79**, 15 (2001).
- [7] K. Ueda, M. Naito, *J. Appl. Phys.* **93**, 4 (2003)
- [8] Y. B. Zhang, H. M. Zhu, S. P. Zhou, S. Y. Ding, Z. W. Lin, J. G. Zhu, *J. Appl. Phys.* **99**, 08M512 (2006).
- [9] A. V. Pogrenyakov, J. M. Redwing, J. E. Jones, X. X. Xi, S. Y. Xu, Q. Li, V. Vaithyanatan, D. G. Schlom, *Appl. Phys. Lett.* **82**, 24 (2003).
- [10] R. Vaglio, M. G. Maglione R. Di Capua, *Supercond. Sci. Technol.* **15**, 1236 (2002).
- [11] Z. Mori, K. Eitoku, T. Doi, S. Koba, Y. Hakuraku, *Physica C* **388**, 115 (2003).
- [12] A. Saito, A. Kawakami, H. Shimakage, Z. Wang, *Supercond. Sci. Technol.* **15**, 1325 (2003).
- [13] A. Mancini, V. Galluzi, U. B. Vetrella, V. Boffa, G. Celentano, L. Ciontea, U. Gamberdella, G. Grassano, T. Petrisor, A. Rufoloni, S. Sprio, M. Vadrucchi, *IEEE Trans. on Appl. Supercond.*, **13**, 2, (2002).
- [14] M. Naito, K. Ueda, *Supercond. Sci. Technol.* **17**, R1-R18, (2004).
- [15] T. He, R. J. Cava, J. H. Rowel, *Appl. Phys. Lett.* **80**, 2 (2002).
- [16] M. Egilmez, L. Ozyuzer, M. Tanoglu, S. Okur, O. Kamer, Y. Oner, *Supercond. Sci. Technol.* **19**, 359 (2006).

*Corresponding author: ozyuzer@iyte.edu.tr